Please cite the Published Version

Additional Information: This is an open access article published in Internet of Things, by Elsevier.

Data Access Statement: The Code scripts for data generation are publicly available in the GitHub repository as part of this research: https://github.com/ken-cisco/ICR-UPCA.cpp.git.

ELSEVIER

Check for updates

Heterogeneous cyber-physical network coexistence through interference contribution rate and uplink power control algorithm (ICR-UPCA) in 6G edge cells

Mfonobong Eleazar Benson [a], Kennedy Chinedu Okafor [b,c,*],
Longinus Sunday Ezema [a], Nkwachukwu Chukwuchekwa [a], Bamidele Adebisi [b],
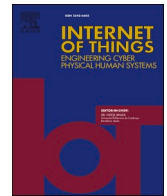Okoronkwo Chukwunenye Anthony [c]

[a] *Department of Electrical and Electronic Engineering, Federal University of Technology, Owerri, Imo State, Nigeria*
[b] *Department of Engineering, Manchester Metropolitan University, M1 5GD Manchester, United Kingdom*
[c] *Department of Mechatronics Engineering, Federal University of Technology, Owerri, Imo State, Nigeria*

ARTICLE INFO

ABSTRACT

Optimizing power control for interference mitigation at the network cell edge is pivotal in enhancing capacity within a heterogeneous cyber-physical infrastructure, such as smart cities, manufacturing, healthcare, energy grids, transportation, and agriculture, among others. In this paper, we consider the intricate dynamics of Internet of Things (IoT) 5/6G edge users, with a particular focus on the Interference Contribution Rate (ICR), where macro and femtocells are critical network infrastructures. Existing approaches has drawbacks such as computational complexity, overhead, among others, co-channel interference. However, to fully address interference challenges from the coexistence of diverse network hierarchies, preserving the Quality of Service for femtocell users is prioritized. The paper concurrently enhances the handoff mechanism of cell edge users in the macro cell network. A two-tier heterogeneous network (HetNet) is utilized to initially assess the contribution of edge user equipment (UE) to interference levels during its active state while quantifying it as ICR. Game theory is used to formulate a cohesive model for the coexistence of macro cell (MUE) and femtocell users (FUE). ICR-based uplink power control and reference signal received quality (RSRQ)-based handoff algorithms are deployed to regulate interference levels and enhance the Signal-to-Interference-Noise Ratio (SINR) of the MUE at the cell edge. This is achieved through coordinated transmit power adjustments by both user types. Results indicate a 6.67 % channel capacity loss (interference tolerance) by the FUE, leading to a 12.5 % improvement, translating to approximately 4 Mbps and 1 Mbps channel enhancements, respectively. The MUE and FUE can effectively coordinate power control with minimal overhead, accepting compromises in network channel quality. This approach facilitates improved MUE data access rates while ensuring the preservation of FUE. We show that interference is successfully mitigated through power control in heterogeneous networks with lower computational complexity.

* Corresponding author at: Manchester Metropolitan University, United Kingdom.
 E-mail address: k.okafor@mmu.ac.uk (K.C. Okafor).

1. Introduction

To enhance traffic capacity in smart infrastructures such as Intelligent transportation systems, smart buildings, smart cities, etc., network densification has become crucial in various 5G/6G powered applications. This has resulted in increased capacity gains, providing more bandwidth within the limited coverage areas of next generation nodes (eNBs). However, this comes with the disadvantage of heightened interference, both in the uplink and downlink [1,2].

In LTE and other legacy networks, the overlapping coverage areas between neighboring eNBs lead to Inter-Cell Interference (ICI), which is unavoidable in 5G to prevent coverage gaps. Moreover, in the 5G network, the rate of ICI is expected to rise as the number of nodes per square area increases due to high network densification requirements [3,4]. Additionally, some proposed power ramping requirements for packet loss mitigation [5] raise concerns about the energy behavior of mobile user equipment in the network.

With the incorporation of femtocells, which are primarily customer-driven [6], it is expected that ICI will be substantial. This necessitates a more effective mitigation approach that is specifically designed to be less complex. Interference in a heterogeneous network is primarily mitigated in two ways: power control and resource coordination between UEs and eNBs or among eNBs in neighboring cells [7].

Most research in this area has employed methods such as Lagrangian maximization functions [8,9], min-median functions [10], Reinforcement Learning [11], Overload Indicator (OI) reports, and programming schemes [12], combined with power control schemes [13,14]. This research has been centered on maximizing cell capacity through SINR improvement without considering self-generated interference to adjacent cells. We seek to delve into the power control method to mitigate interference at the cell edge in a heterogeneous network.

While several researchers have explored power control in homogeneous and heterogeneous network structures, focusing on either the downlink or uplink, and addressing user-specific or neighbor-aware interference mitigation, there are still gaps in the existing body of work. Power control (PC), whether Open Loop (OL) or Closed Loop (CL), has remained a standard, with CL-PC demonstrating promising advantages over OL–PC in a closed system. OL–PC is applied to initiate a connection to a network by the UE, while CL–PC is designed to maintain transmit power in sync with the base station's requirements. Some diversification of these legacy approaches has been attempted to achieve other forms of power control, as seen in [10,15], where in-out interference was considered to determine OL–PC parameters. OL–PC parameters are used to initiate connections but lack the ability to maintain a fair control approach. Additionally, using OL–PC instead of CL-PC to achieve lower power output has been explored. However, no OL–PC approach has demonstrated significant gains in a coordinated or shared environment, as users tend to act selfishly.

Programming approaches have also been employed [13,14] applying utility maximization functions and geometric programming (GP) to achieve power control for rate maximization, yielding improved results. However, these approaches often overlook the impact of other Key Performance Indicators (KPIs) on the network. Another approach involves using the Overload Indicator (OI) as a KPI to achieve power control. In [10,15], the focus was on reducing cross-tier interference, recognizing that different infrastructures share the same frequency bands [16]. The OI was employed to control UE's transmit power. Since OI is a general metric, it cannot be applied specifically to individual interferers but rather across the entire network. This may not be effective in a small cell within a HetNet for specific UEs.

Considerable research has been conducted to determine the tolerable transmit power of femtocell users (FUE) within the macro cell coverage to avoid cross-tier interference, as demonstrated in [17–19]. Improved results were achieved when considering macro cell users (MUE). However, it is apparent that interference suffered by FUEs was not considered, which also influences their power requirements. There has yet to be a power control algorithm that considers handover as an option in extreme cases when desired results cannot be achieved. Interference has remained a leading factor in bandwidth underutilization, and in 5G-NR, it remains a major issue, affecting data quality and channel quality. High data rate requirements, network densification, and limited energy sources pose challenges for efficient energy management, necessitating effective power management in the uplink.

In this paper, we employed optimal power control for a 5G/6G edge user service device and proposed Interference Contribution Rate (ICR) to limit neighbor interference rates by continuously evaluating and applying corresponding power control parameters. In this process, Self-generated interference is considered while recommending handover in cases where power control becomes unfeasible due to poor channel quality, and deviation from the expected signal strength.

The established concerns derived in this paper are summarized below.

1. Wireless Communications and Network Densification:

   How can we mitigate interference effectively in high-density 5G/6G networks to ensure seamless connectivity for applications like smart health and autonomous vehicles?

2. Inter-Cell Interference Management:

   What novel approaches can be developed to address Inter-Cell Interference (ICI) in 5G/6G networks, considering the unique challenges posed by network densification and overlapping coverage areas?"

3. Power Control Strategies for Heterogeneous Networks:

How can power control strategies be optimized to balance SINR improvement and interference reduction in heterogeneous networks, considering user-specific needs and neighbor-aware interference mitigation?

4. Power Control Algorithm Diversity:

   What innovative techniques can be explored to diversify power control algorithms, particularly in coordinated or shared network environments, to promote fairness and mitigate selfish user behavior?

5. Multi-KPI Power Control:

   How can power control algorithms be enhanced to consider multiple Key Performance Indicators (KPIs) beyond rate maximization, ensuring a holistic network performance improvement while mitigating interference?

6. Handover and Extreme Cases in Power Control:

   What strategies can be developed to handle power control in extreme cases where conventional methods fail due to poor channel quality, with a focus on alternative options like handover, especially in small cell HetNets?

These research questions narrow into the complexities of 5G/6G edge communication network, power optimization, and interference management, while providing opportunities for in-depth industry research and innovation in the field.

The research major contributions are summarized below:

1. To quantify Interference Contribution Rate (ICR) for 6G edge user equipment (UE) in heterogeneous networks. This represents a novel approach to understanding and managing interference in such networks.
2. To derive a harmonized coexistence model with game theory between macrocell (MUE) and femtocell users (FUE) while addressing interference challenges in heterogeneous networks.
3. To achieve an improved Signal-to-Interference-plus-Noise Ratio (SINR) for MUEs at the cell edge. This is carried out through coordinated transmit power adjustments based on ICR. This contributes to improved data access rates for macrocell users.
4. Quantify the trade-off between interference tolerance and channel capacity for FUEs. We showed that a controlled compromise of interference tolerance can result in substantial channel improvements for both user groups, (i.e., Interference Tolerance Trade-off)
5. Employ a coordinated power control strategy that allows MUEs and FUEs to work together with minimal overhead, (i.e., Minimal Overhead Coordination). We represented a practical approach to interference management in heterogeneous networks.
6. Demonstrate and validate power control optimization and handoff schemes. We showed how these effectively mitigates interference in heterogeneous networks, contributing to better coexistence and improved network performance.

2. Related works

In this section, this paper will review the significant obstacles that have brought about for edge communications in terms of network capacity, data speed, and energy efficiency by the rapid expansion of edge-device data services. As a result, the authors [20] notes that current mobile communication networks are under tremendous strain. In response to the increasing need for mobile services, there has been a lot of focus on the 5G mobile communication in both industry and academics. Numerous novel approaches and technological advancements have surfaced, such as dense cellular HetNet [21], mmWave [22], and massive MIMO [23]. The authors verified that the use of space multiplexing, and massive MIMO technology have improved data transmission rates and spectrum efficiency. The authors [20] has explored gigahertz-level transmission bandwidth using millimeter wave frequencies but in contrast to mmWave and massive MIMO, which mainly benefit the physical layer, HetNet [21], which uses densely deployed tiny cells, effectively boosts mobile data speeds and system capacity. Deploying a lot of 5G has intensively become an effective way to achieve seamless coverage and enough network capacity in the hot spots area. This is because a lot of low power small cell facilities, like relay nodes, micro base stations, Femto cells, and Pico cells, can divert load and increase network capacity [20]. Table presents a summary of various optimization schemes and their trade-offs.

The major limitations of most related efforts in literature include challenges such as co-channel interference affecting IoT traffic, power drain in intercell coordination, and difficulties in managing beamforming, interference, and resource allocation for optimal efficiency and security in various communication scenarios.

3. Environment and experimental methodology

In this paper, the following materials are utilized to re-design the model in [30]:

 i. **Hardware:** The Umidigi A9 Pro smartphone featuring a Mali-G72 GPU and a CPU with eight cores, operating at a minimum and maximum frequency of 793 MHz and 1807 MHz, respectively.
ii. **Software:** Various software tools were employed, including Battery Gauge, AccuBattery/Battery Guru, InWare, NetWard/NetMonster, MATLAB software R2020b, and Google Maps.

This paper designed a heterogeneous network environment encompassing both a macro cell and a small cell (femtocell) with a shared interest in cellular coverage, as illustrated in Fig. 1. The small cell (FeNB) was deployed randomly, simulating user-deployment, thus precluding coordinated or planned (uniform) deployment. This setup allowed us to analyse power performance and resource utilization between the Macro User Equipment (MUE) and Femto User Equipment (FUE). The aim is to develop a game theory-based approach for improved interference management, ultimately leading to system optimization.

3.1. System model

Considering a two-tier heterogeneous network (HetNet), where a femtocell (FeNB) is under-laid within the coverage area of the macro-cell as shown in Fig. 1. The whole network is assumed to share the whole spectrum (macro and femtocell), meaning a reuse factor of one ($k = 1$), as it is the proposition in fifth-generation new radio (5G-NR), due to the scarcity and cost of spectrum, also, the one reuse factor is very essential to spectrum efficient utilization. The HetNet under consideration will consist of one macro cell (eNB) and a small cell (1-FeNB).

3.2. System assumptions

  i. That FeNB is randomly distributed.
  ii. The sets of UEs $M = \{1, 2, 3, \ldots, m\}$ served by the eNB, and the sets of FUEs $F = \{1, 2, 3, \ldots, f\}$ served by the FeNB are all randomly deployed.
  iii. That each UE can only associate with one serving node (FeNB or eNB) at a time,
  iv. That all UEs initially transmit with minimum power (P_{min}).

The received uplink SINR (ɣ) for the UEs served by the eNB (MUE) can be expressed as in Eq. (1) while assuming the non-existence of intracell interference [20,21].

$$\gamma_M^m = \frac{P_{m,M}^{tx} G_{m,M}}{\sum_{f=1}^{F} P_{f,F}^{tx} G_{f,F} + \sigma_p^2} \tag{1}$$

The received uplink SINR (ɣ) for the UEs served by FeNBs can be expressed as in Eq. (2) [20,21].

$$\gamma_F^f = \frac{P_{f,F}^{tx} G_{F,f}}{\sum_{m=1}^{M} P_{m,M}^{tx} G_{m,M} + \sigma_p^2} \tag{2}$$

Where γ_M^m and γ_F^f are the SINR or macro (eNB) and small cell users (UEs) respectively, $P_{M,m}^{tx}$ and $P_{F,f}^{tx}$ are transmit power of UEs served by eNB and FeNBs within the eNB coverage area respectively, $G_{M,m}$ and $G_{F,f}$ are the channel gain between FUE to FeNB and MUE to eNB while σ_p is the noise spectral density of the channel. Both MUE and FUE in the network will be taken into account by the power control policy as presented in Eq. (3).

The total capacity within a channel is given as

$$\varsigma = Log_2\left(1 + \gamma_F^f\right) + Log_2\left(1 + \gamma_M^m\right)$$

$$\varsigma = Log_2\left(1 + \frac{P_f h_f^2}{\sum_{k=1}^{U_m} h_m^2 P_m + \sigma^2}\right) + Log_2\left(1 + \frac{P_m h_m^2}{\sum_{i=1}^{U_f} P_f h_f^2 + \sigma^2}\right) \tag{3}$$

Where h_f^2 and h_m^2 are sub-channel gain, P_f and P_m are transmit power for macro and femtocell users respectively, and σ^2 is the noise
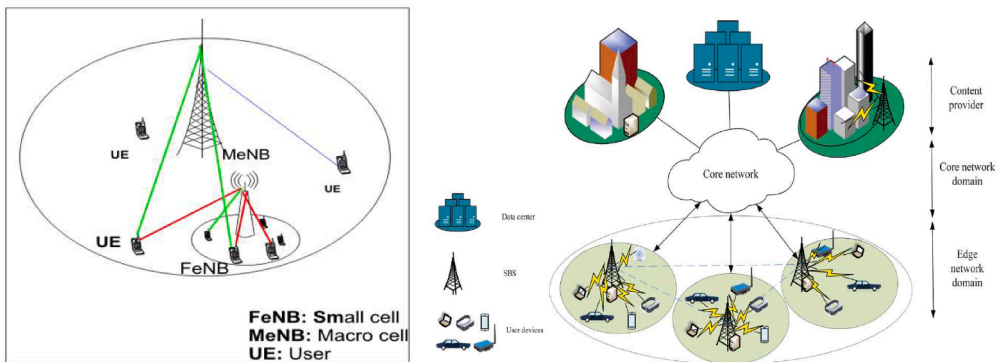

Fig. 1. HetNet system model with 6G edge network domain [30].

spectral density. Gong et al. [22] attempted to solve this problem but ended up with a different solution from what is obtained.

In a non-corporative scenario, the UEs in the network are assumed not to communicate with one another. The systems make their individual decisions without the influence of the other. Therefore, the decision to be taken is said to be positive only when such a decision attains the Nash equilibrium; this is a decision that is constrained with the lowest consequence no matter the combination of their outcomes. That is, no matter the decision taken by user A, the outcome of user B's decision will still attract low consequences called the penalty.

We need to prove concavity by taking the second derivative of the function $f(P_f)$.

For $\varsigma = f(P_f)$

If $f'(P_f) > 0$ the second derivative is positive and the function is said to be concave upward, else if $f'(P_f) < 0$ the second derivative is negative and the function is said to be concave downward.

$$\frac{\partial \varsigma}{\partial P_f} = \frac{\partial}{\partial P_f}\left[Log_2\left(1 + \frac{P_f h_f^2}{\sum_{k=1}^{U_m} h_m^2 P_m + \sigma^2}\right) + Log_2\left(1 + \frac{P_m h_m^2}{\sum_{i=1}^{U_f} P_f h_f^2 + \sigma^2}\right)\right]$$

$$= -\frac{P_m h_m^2 h_f^2}{\left(P_f h_f^2 + \sigma^2 + h_m^2 P_m\right)\left(P_f h_f^2 + \sigma^2\right)} + \frac{h_f^2}{P_f h_f^2 + \sigma^2 + h_m^2 P_m}$$

The second derivative of the function yields the equation

$$\frac{\partial^2 \varsigma}{\partial P_f^2} = -\frac{h_f^4}{\left(P_f h_f^2 + \sigma^2 + h_m^2 P_m\right)^2} + \frac{P_m h_m^2 h_f^6}{\left(\left(P_f h_f^2 + \sigma^2 + h_m^2 P_m\right)\left(P_f h_f^2 + \sigma^2\right)\right)^2}$$

Since $\frac{\partial^2 \varsigma}{\partial P_f^2} < 0$, i.e. negative, the function is assumed to be concave

Using the gradient method for optimality, we equate $\frac{\partial \varsigma}{\partial P_f}$ to zero to yield the optimal power for UEs served by FeNB; (FUE).

$$-\frac{P_m h_m^2 h_f^2}{\left(P_f h_f^2 + \sigma^2 + h_m^2 P_m\right)\left(P_f h_f^2 + \sigma^2\right)} + \frac{h_f^2}{P_f h_f^2 + \sigma^2 + h_m^2 P_m} = 0$$

$$P_f^2 h_f^4 + P_f\left(2 h_f^2 \sigma^2\right) + \sigma^4 - P_m^2 h_m^4 = 0$$

Solving for P_f:

$$\left|P_f^*\right| = \frac{-2\left(h_f^2 \sigma^2\right) \pm \sqrt{\left(2\left(h_f^2 \sigma^2\right)\right)^2 - 4(h_f^4(\sigma^4 - P_m^2 h_m^4)}}{2 h_f^4} \tag{4}$$

4. Interference models

As it is with the 5G/6G network as proposed by the 3GPP, a reuse factor (K) of one is necessary for enhanced bandwidth utilization as against multiple reuse factors used in legacy networks. It is expected that two (2) forms of interference will exist in the model presented based on the uplink channel;

 i. Interference from FUE to MeNB
ii. Interference from MUE to FeNBs

4.1. Edge UE interference contribution rate (ICR)

The interference contribution rate (ICR) of UEs is taken as the ratio of the interference power caused by the neighboring UEs to the sum of reference signal received power (RSRP) of every active UE towards the serving eNB and can be obtained as in Eqs. 4(a and b).

$$\psi_{FUE,MUE} = \frac{\sum_{i=1}^{N} P_i^{tx} G_i}{\sum_{j=1}^{M} P_j^{tx} G_j} \tag{4a}$$

$$\psi_{FUE,MUE} = \frac{\sum I_{eff}}{RSRP_r} \begin{cases} < 1.5, \Delta^+, \mathscr{L}^+ \\ \geq 1.5, \Delta^-, \mathscr{L}^- \end{cases} \tag{4b}$$

Where,

ψ: ratio of interference contribution

RSRP: specific users' received signal power

I_{eff}: Effective interference

P_i^{tx} and P_j^{tx}: transmit power of femtocell and macro cell user

G_j and G_i: channel gain

The ICR value tells the extent to which the user under consideration is suffering interference distortions from other users. This gives a sense of direction to either increase or decrease the transmit power (according to standards) of the sufferer or the interfere respectively, while Eq. (5) determines the expected fractional change of the transmit power to achieve the target SINR level.

$$\mathscr{L}_{F,M} = \frac{\beta(N + I_{f/m})}{2.5119} \tag{5}$$

The expected change in transmit power is obtained from Eq. (6), which gives the limit to which the transmit power can be changed.

$$P_{req} = \mathscr{L}\left[\frac{2.5119}{N + I_{f/m}}\right](N + I_{f/m}) = \frac{\beta(N + I_{f/m})}{2.5119} \tag{6}$$

Where;

β: difference in SINR state

N, $I_{f/m}$: Noise and sum of effective interference of MUE/FUE

$\mathscr{L}$: Fractional Tx power incremental/decremental ratio

P_{req}: Required additional fractional Tx power to SINR threshold levels.

N is the sum of MUEs in the FeNB cell range i

M is the sum of FUEs in the interfered cell j, while P and G maintain their usual meaning.

The amount of interference experienced increases as the nature of service used differs within the cell range.

4.2. Dynamic power offset

The power utilization for UEs at the cell center and those at the cell edges need to be balanced systematically to maintain some level of acceptable overall quality in the network. Therefore, the interference rate experienced by the FeNBs must be examined in a bid to identify interferers and apply the power control schemes as appropriate. It is logical to apply power control on interferes and not just on the interfered UEs, as this should lead to controlling overall power offset in the network. The amount of interference that a UE can tolerate (known as effective interference) can be determined using Eq. 7.

$$M_I = RSRP_{f,k} - I_{t,k} - N_p \tag{7}$$

Where;

M_I is the maximum tolerable interference

$RSRP_{f,k}$ is the serving UE's RSRP on RB k

$I_{t,k}$ is the total interference received in resource block k

N_p is the spectral noise power

Minimum SINR with reference to M_i from Eq. (7) is given in Eq. (8) as

$$SINR_{min} = RSRP_{f,k} - M_I - N_p \tag{8}$$

4.3. UE system classification

The UEs are classified based on application as Real-Time (RT) and non-Real-Time (nRT). The RT service UEs require better SINR than those of the nRT, therefore, the applied Power Control (PC) will be expected to be service-dependent, as the SINR of UEs within the network will vary depending on the overall power utilization expected of the FeNB to control interference to the MeNB is given as;

$$SINR_{nRT} < SINR_{RT} \tag{9}$$

Although, the SINR can be kept equal for both RT and nRT applications in situations where RBs can be dynamically allocated. Allocating more RBs to a UE based on data rates or capacity required, even when the dynamic allocation of more or fewer RBs is possible; will result in dynamic power allocation also.

4.4. Cell edge user identification

It is important to identify the UEs at the far end of the cell coverage area, as their channel characteristics differ from those at close range to the eNB. The cell edge users are characterized by low SINR, and RSRP or RSSI; depending on the network or service under consideration. The cell edge UEs and the out-of-range UEs can be determined and identified using Eqs. 10 and 11 as;

$$SINR_{UE,i} \leq SINR_{thresh} \tag{10}$$

$$SINR_{UE,i} \ll SINR_{thresh} \tag{11}$$

When the UEs' SINR is less or equal to the minimum achievable SINR at power ($< P_{max}$) within the cell, the UE is treated as a cell edge user, and when the SINR of a UE is far less than the cell threshold SINR (minimum allowable SINR), the UE is assumed to be out of range.

4.5. ICR-based uplink power control algorithm

In this subsection, we assumption:

i. FeNB is static while FUE has limited mobility (almost static) due to the small coverage of the network (10 m).
ii. Tx Power of both FUE and MUE is distinctive when there is a service change (real and non-real-time).

Algorithm 1 is part of larger Cyber-physical system for managing interference and controlling the uplink transmission power of user equipment in a Femto Cell environment. The specific details of the Equations and parameters focused on maintaining the desired signal quality and interference control for both MUEs and FUEs. Below is the breakdown of the key steps in Algorithm 1:

Initialization:
The algorithm starts with some initialization steps, decomposed into layers below.
Algorithm Flow:

---

i. For each MUE in the Femto Cell (FeNB):
   - Compute a value called P_f^* using Eq. (4).
   - Compute the ICR for the MUE and FUE, as well I_Eff.
ii. Check if the calculated ICR for FUE and MUE is less than 1.5. The ICR likely measures the quality of the uplink signal.
iii. **If** ICR is less than 1.5, it enters an "ICR Table" check:
   - **If** ICR Table is equal to Δ_tx^+ (not defined in the provided code), **then:**
   - Compute P_req and increment it by +4 dBm (decibels relative to 1 milliwatt).
   - Update the ICR Table and Power records.
iv. **If** ICR Table is not Δ_tx^+ (the "else" condition), **then:**
   - Update the ICR Table and indicate Δ_tx^- (again, not defined in the code).
   - Recommend Handover (likely a suggestion to switch to a different cell or access point).
v. **If** the ICR is greater than or equal to 1.5, **then** it implies a more stable user:
   - Update Power records and ICR Offset.
   - Indicate that it's a stable user.

End

Algorithm 1 show the ICR-based Uplink Power Control. Assuming a femtocell infrastructure at the cell edge of an active macro cell. It is required that the femtocell system (FeNB) computes its allowable maximum transmit power using the optimization equation derived P_f^*. The resultant value obtained using this equation is the maximum allowable. According to 3GPP, every UE on the LTE-A network begins transmission using the lowest possible transmit power and increment by ± 4 dBm to expected levels, hence, the ICR is used to determine safe transmit power levels due to effective interference suffered by the FUE on their respective channels. Where an

Algorithm 1
ICR-based uplink power control algorithm.

	Inputs: Total interference by MUE, Indoor Path gain, Min. SINR, MUE Tx range
1	**Outputs:** ICR, FUE Tx safe range
2	Initialization…
3	**For** all MUE in FeNB Cell
4	**Do:** Compute P_f^* Using Eq. (3.4)
5	**Do:** Compute ICR for MUE and FUE, and I_{Eff}
6	**IF** $ICR_{FUE, \ MUE} < 1.5$
7	**Do:** Check ICR Table
8	**IF** $ICR_{Table} = \Delta_{tx}^+$
9	**Do:** Compute P_{req} and increment by +4 dBm
10	**Do:** Update ICR_{Table} and Power records
11	**Else**
12	**Do:** update ICR_{Table} and Indicate Δ_{tx}^-
13	**Do:** Recommend Handover
14	**Else**
15	**Do:** Update Power records and ICR Offset
16	**Do:** Stable User
	End

ICR ratio is greater than 1.5, it implies that the user is affected and degraded by interference and either requires higher transmit power or their interferers require and downward review of transmit power.

Alternatively, assuming a femtocell infrastructure at the cell edge of an active macro cell. It is required that the femtocell system (FeNB) computes its allowable maximum transmit power using the optimization equation derived P_f^*. The resultant value obtained using this equation is the maximum allowable. According to 3GPP, every UE on the LTE-A network begins transmission using the lowest possible transmit power and increment by ± 4 dBm to expected levels, hence, the ICR is used to determine safe transmit power levels due to effective interference suffered by the FUE on their respective channels. Where an ICR ratio is greater than 1.5, it implies that the user is affected and degraded by interference and either requires higher transmit power or the interferers require a downward review of the transmit power. The ICR Power table is used by MUE/FUE to determine expected adjustments in Tx power.

Assumption:

The FUE are already active and connected indoors. The MUE at the cell edge initializes (starts) the connection protocol with eNB. After gaining connection using the lowest possible transmit power, the FeNB and eNB compute the ICR of both networks as MUE may be suffering from low SINR. If the ICR of MUE is less than 1.5, the eNB checks the interference impact on FeNB before recommending power adjustments of MUE while referencing the ICR table of FeNB as given in Table 1 (a–c). If the ICR table for FeNB indicates $\Delta_{tx}^-/\Delta_{tx}^+$ in the balance column, it means that the SINR of FUE is above its set threshold for the current service deployed and can be adjusted both ways (up/down). Else, if the ICR balance column of the FUE shows a Δ_{tx}^+ only, then it implies that FUE is operating at its SINR threshold and has low interference tolerance. This limits any change in transmit power of the MUE or FUE, where MUE cannot do with its present SINR, it is regarded as out-of-range and recommended to handoff as shown in Fig. 2.

In the presence of 'Δ_{tx}^+' in the balance column, it implies that the UE has no room to decrease its transmit power. It therefore implies that the UE is currently being served at its threshold SINR or minimum detectable signal (MDS) strength. Whereas, when 'Δ_{tx}^-' is shown in the balance column, which implies that the UE has the privilege of decreasing its power level further from its current state. Where an FUE indicates Δ_{tx}^+ at the same time with MUE, it means that the SINR of the MUE cannot be improved by power control, hence, vertical

Table 1
Related efforts, techniques, domains, metrics and limitations.

References	Optimization techniques	Application domain	Merits	Limitations
Shen, et al. [20]	ICR-small on/off switching and Network Adjacency matrix	Heterogeneous 5G Networks.	Less computational complexity	Co-channel interference can mask IoT traffic and power efficiency
García-Morales et al. [24]	Fractional & soft Frequency reuse	Multi-cellular Networks	Inter-cell interference coordination	Power drain due to active Edge intercell interference coordination
Budhiraja et al. [25]	Two-phased Tactile Internet driven delay assessment	Two-hop cooperative Communication	D2D transmitter's power is optimization via low-complexity convex approximations	Cell edge users Throughput is affected due to cochannel interference mitigation overhead.
Xue et al. [26]	Fractional programming & minimum mean square error criterion.	mmWave Reconfigurable intelligent surfaces communications (RISC)	Low complexity optimization algorithm	Issues of beamforming optimization, interference management, energy efficiency, reconfiguration coordination, hardware complexity, user mobility adaptation, scalability, and security.
Subhash et al. [27]	Channel statistics-MIMO with asymptotic deterministic counterpart of the minimum SINR	RISC	lowers the quantity of controlling data & computational complexity needed to update the phases between the RIS and BS.	Difficult to properly assess its limitations and generalizability due to the absence of important technical details, context, and wider applicability.
Shi et al. [28]	Fractional power control & max-min power control algorithm	Cell-free MIMO and RIS future beyond-fifth generation networks	Optimised electromagnetic interference degradation of spectral efficiency	Difficulties in managing channel correlation, interference, channel estimation, and resource allocation while maximizing energy efficiency and security. These are encountered in a spatially correlated RIS-aided CF massive MIMO system with multi-antenna access points over spatially correlated fading channels.
Li et al. [29]	Ergodic sum-rate of the non-orthogonal multiple access uplink simultaneous transmitting and reflecting reconfigurable intelligent surface	RIS	Optimised electromagnetic interference degradation of spectral efficiency	Channel estimation errors not reliably fixed
Liming et al. [30]	Joint Coded caching with maximum distance separable & Base station sleeping.	6G Edge Networks	Edge caching offers huge potential for energy savings.	Computational complexity in DPSO not addressed
		6G Edge Networks	Lower computational complexity,	

handover is recommended. Table 2 (a–c) shows the overall ICR table.

a. FUE Overall ICR Status

Add	Subtract	Balance	
Δ_{tx}^+	Δ_{tx}^-	Δ_{tx}^+	Δ_{tx}^-

a. MUE: Application Status for increased Tx power

Real-time	Non-Real-time		Balance
Δ_{tx}^+	Δ_{tx}^+	Δ_{tx}^-	Δ_{tx}^+

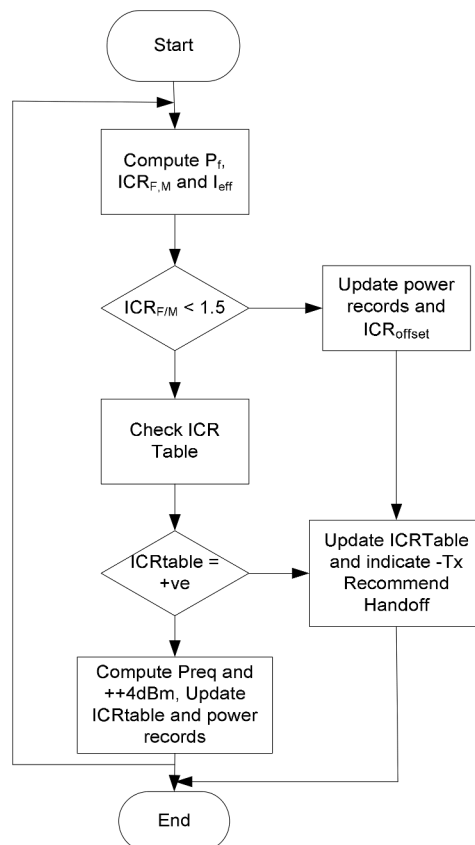a. MUE: Application Status for decreased Tx Power

Fig. 2. ICR - based UPC procedure.

Table 2
Model nomenclatures.

Symbol	Meaning
γ_M^m, γ_F^f	Macro and Femtocell UE SINR
$P_{m,M}^{tx}$, $P_{f,F}^{tx}$	Macro and Femtocell UE Tx power
ς	Shared channel capacity
h_f^2, σ^2	Shared channel gain and noise power
P_f^*	Femtocell UE optimized Tx power
ψ, I_{eff}	ICR ratio and effective interference
$\mathscr{L}_{F,M}$, β	Fractional Tx power increment (+ or -) and state difference of SINR
$I_{f/m}$	Interferes due macro or femtocell UE
M_I, $I_{t,k}$	Interference tolerance and total received interference

Real-time	Non-Real-time		Balance
Δ_{tx}^-	Δ_{tx}^+	Δ_{tx}^-	Δ_{tx}^-

4.6. Signal quality-based handoff algorithm

Since power control has its limitation to channel response, it is pertinent to consider handover as an option at critical points (where power control is not feasible). Handoff has been in practice in mobile communication to aid mobility and continuity of service. Algorithm 2 focuses on real-time users requiring better channel quality for deployed services and reducing interference within femtocell coverage areas. Classical handoff algorithms use signal strength to determine UE movement, but considering channel quality as an indicator is essential, as signal quality and strength can sometimes be mutually exclusive. Handoff scheme currently implemented are dependent on the signal strength of both service-providing infrastructures. Handoff mechanism used in our 6G edge cells (MIMO-networks), is designed such that the edge UE receiver can be connected to antennas from both nearby cells' base stations to get the best performance possible during handoff (i.e., multicell handoff). The system with weaker signal handoffs to the adjacent system with a stronger signal, while hoping that the user is moving toward the system with a stronger signal. In this research, it was realized that slow-moving nodes experience scenarios where the signal strength may be poor, but with better quality. In this case, the conventional handoff algorithm ignores the situation for the fact that the signal strength is stronger. Although handoff based on signal quality seems more complex when compared with signal strength, signal quality remains more energy efficient when deployed on slowly mobile or static nodes at the cell edge. We later investigated the computational complexity, and the findings show that in the situation of high spatial correlation, the multicell handoff improves average CPU throughput with lower CC.

Considering Algorithm 2, RSRQ stands for Reference Signal Received Quality, M_th is a threshold value for some parameter M_i, and SINR stands for Signal-to-Interference-plus-Noise Ratio. The RSRQ-Based Handoff Algorithm is another layer of the Cyber physical communication system for the edge cellular network. It seems to be a handoff algorithm for Real-Time Mobile User Equipment (MUE) in a Femtocell (FeNB) cell. Here's a step-by-step breakdown of how the Algorithm 2 works:

Input Parameters:

- M_th: A threshold value for some parameter M_i.
- SINR_th: A threshold value for Signal-to-Interference-plus-Noise Ratio.
- RSRQ_th: A threshold value for Reference Signal Received Quality.

Algorithm Steps:

1. Loop through all Real-Time MUEs in the Femtocell (FeNB) cell.
2. In real time individual MUE, calculate M_i, $SINR_{UE}$, and $RSRQ_{UE}$, $RSRQ_{adj}$.

Algorithm 2
RSRQ-based handoff algorithm.

1:	**INPUT:** M_{th}, $SINR_{th}$, $RSRQ_{th}$
2:	**Initialize** minimum mean square error (MMSE) $\mu_\delta()$
3:	**For** all Real-Time MUE in FeNB Cell
4:	**Do:** Compute M_i, $SINR_{UE}$, and $RSRQ_{UE}$, $RSRQ_{adj}$
5:	**IF** Mi > Mth and $SINR_{UE} < SINR_{th}$
6:	**Do:** Compare RSRQue to RSRQad
7:	**IF** RSRQue < RSRQadj
8:	**Do:** Initiate Handoff
9:	**Else** Return to power control
10:	**Else** Return to power control
End	

3. With control decision mapping check for critical thresholds and modulate effectively.
4. Compare and further initiate active handoff for power control
5. If M_i is not greater than M_th or if SINR_UE is not less than SINR_th, there is no need for a handoff or power control, so the UE continues operating in the current cell.

As shown above, Algorithm 2 depicts the RSRQ-based handoff scheme. The handoff algorithms currently implemented are dependent on the signal strength of both service-providing infrastructures. The system with weaker signal handoffs to the adjacent system with a stronger signal, while hoping that the user is moving toward the system with a stronger signal. In this research, it was realized that slow-moving nodes experience scenarios where the signal strength may be poor, but with better quality. In this case, the conventional handoff algorithm ignores the situation for the fact that the signal strength is stronger. Although handoff based on signal quality seems more complex when compared with signal strength, signal quality remains more energy efficient when deployed on slowly mobile or static nodes at the cell edge.

The real-time user is determined by the interferer with the highest ICR value whose SINR is less than the SINR threshold. As the network routinely checks for interferers and reports by updating the ICR table, the highest interferers are treated for handoff operation as given in Fig. 3. The handoff process initializes only when there is an interferer whose power requirement cannot be controlled within the limited resources. According to the algorithm presented above, the process initializes by updating its measurements on SIR, RSRP and RSRQ of its user and adjacent channels (if available). The SIR value of UE is compared to the set threshold and the M_i value is evaluated as given in Eq. 7 to consider the tolerance level of FUE. If SIR is below the threshold and the Mi is above tolerable levels, the RSRQ of the user and the adjacent channel is compared and evaluated. If the RSRQ of the user is less than the adjacent RSRQ, a handoff request will be issued and processed, otherwise, the process is returned to the power control stage.
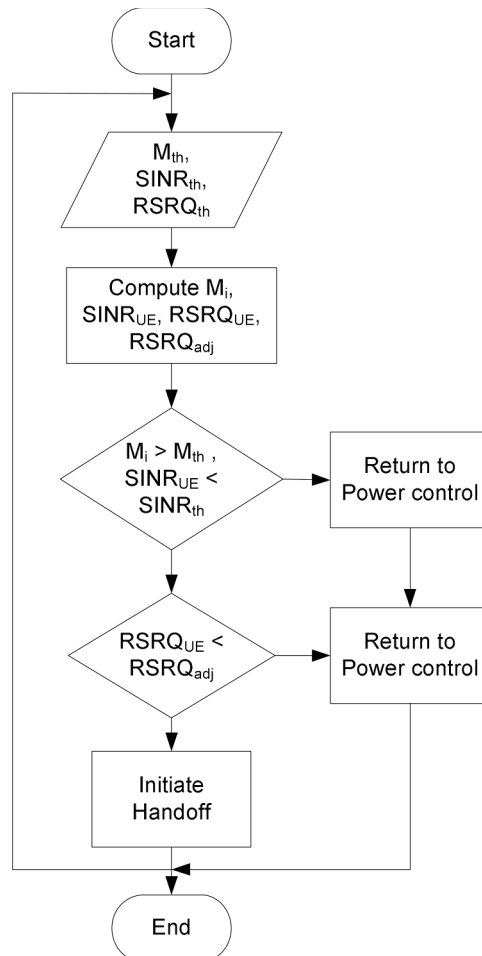

Fig. 3a. Signal quality-based handoff procedure.

5. Computational complexity (CC)

A major challenge in 5G/6G edge cells is the computational complexity of the massive MIMO systems discussed previously. The CC of a hand-off mechanism refers to the number of computational resources required to execute the necessary tasks when transitioning a connection or device from one access point or network node to another seamlessly. The complexity varied based on the handoff technique for edge device stream exchanges in 6G edge cells. For the 6G edge cell infrastructure, first, the identified factors affecting the established complexity include algorithmic decision-making, information exchange between node devices, access points, resource management during hand-offs, and the timing and efficiency of the hand-off process. These elements impact the computational traffic workload involved in initiating seamless transitions between network cell connections.

Now, the CC is described in terms of Big O notation. This characterizes the hand-off scalability considering the input data size for 6G Cells. The number of edge nodes and network-state conditions are considered also. The hand-off mechanisms had on-demand complexities described as $O(1)$ (constant time), $O(\log n)$ (logarithmic time), $O(n)$ (linear time), as well as higher complexities $O(n^2)$ (quadratic time), depending on the specific edge device on-demand tasks and the efficiency of the algorithm. Since the complexity varies across different hand-off schemes and network types, this paper employed low computational complexity scheme, (i.e., approximate matrix conversion) to ensure seamless transitions without introducing significant delays and overhead in the network. The proposed hand-off mechanism offers balance efficiency, accuracy, and responsiveness while minimizing computational overhead. Also, due to the use of approximation algorithm for handoff, the CC reduced from order $\vartheta(M^3)$ to order $\vartheta(M^2)$. The approximation algorithms have less CC than the other handoff proposed algorithms [31].

Considering the 6G MIMO system, we used the work [31] to compare high-CPU dimensional matrix computations during handoffs. For 6G edge cells, minimum mean square error (MMSE) algorithm prioritize low complexity, hence three distinct handsoff mechanisms are discussed viz: the proposed approximate matrix conversion MMSE (HO-AMCMMSE), iterative MMSE (HO-IMMSE) and matrix gradient search MMSE (HO-MGSMMSE). The CPU utilization rates during various handover processes were observed in Fig. 3b. During HO-IMMSE, the CPU usage peaked at 85.42 %; HO-AMCMMSE offered 77.78 % usage, while HO-MGSMMSE offered 81.93 % CPU utilization. The overall CC of an inverse matrix Handoff-mechanism decreases when compared to the usual iterative, and matrix gradient search schemes as shown in Fig. 3b. However, its necessary to note that the proposed handoff-mechanism is designed in such a way that at higher SNRs, the bit error rate is reduced. Hence, the CC in the coding and decoding blocks are optimally reduced. This suggests that in large-scale networks, the handoff-based approach is more scalable.

The significance of Fig. 3b is that with the reduced CC, it took less than 4 s to evaluate channel quality based on error rate, and coding scheme correction as scheduled to make a handoff recommendation. However, the parameters required for this process are basic entries already defined within an edge cell system. In this handoff-mechanism case, the uplink channel quality is evaluated continuously (periodic, aperiodic, or on request) during active and standby mode by the 6G base station. With reduced CC, there was minimal additional energy demand placed on the mobile edge equipment. It's worth noting that the user equipment (UE) concurrently measures and reports downlink channel quality as part of the channel state information (CSI), crucial for informing the 6G base station's decisions regarding power control and other parameter adjustments.

6. Results

6.1. New power control algorithm implementation

First, we used the simulation parameters [30] to implement our model. This was considered to provide a guide between the Femto and Macro cell user coexistence in transmit power control during real-time and non-real-time service deployment. Fig. 4 shows improved interference levels leading to an optimized FUE transmit power based on collaborative power-interference ratios, while the FUE SINR in this case is protected from aggressive greedy MUE. The FUE data shows a consistent positive trend, with each interference value generally increasing by around 0.9–0.97 from the previous value. This suggests that the number of Femtocell users is increasing steadily over time. Similarly, the MUE data also shows a positive trend, with each increasing by approximately 0.9–0.97. Both cell
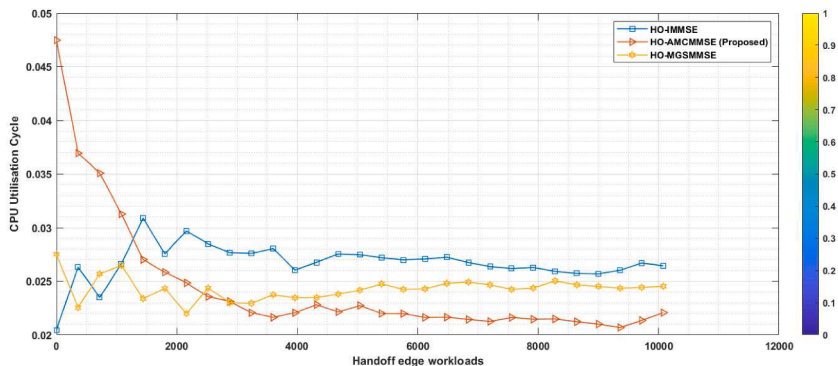

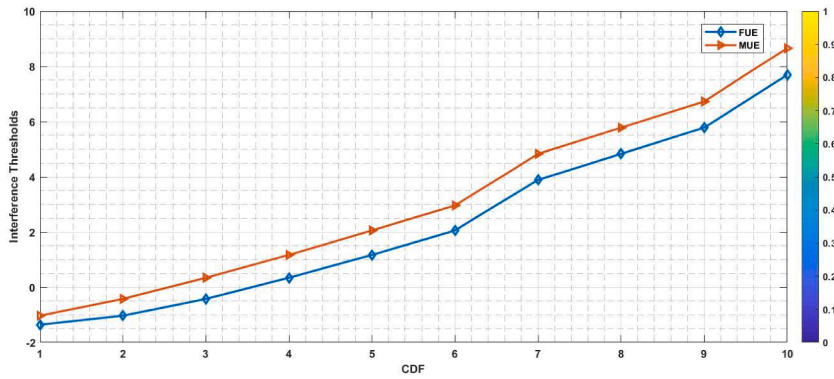**Fig. 3b.** Handoff computational complexity.

Fig. 4. FUE optimized power.

users are experiencing a positive trend, with the number of users increasing over time.

6.2. Interference between MUE and FUE coexistence

The FUE interference towards the MUE as presented in Fig. 5 was observed to be minimal at lower power levels up to 18 dBm, whereas, the MUE interference was high all through to 23 dBm which is the maximum allowed for every UE within the network. It is interesting to note that the algorithm does not allow the FUE transmit power to rise beyond 22 dBm while the MUE can attain such power levels and even more. The MUE data shows a consistent positive trend, with each value generally increasing by around 7.67–12.08 from the previous value. This suggests that the number of Macro Cell users is steadily increasing over time. At a transmit power of 15 dBm, the FUE can go almost unnoticed in interference by the MUE as this generates a very low level of interference signal allowing for better rates on the MUE. Therefore, aiming the transmit power of the FUE at lower rates while protecting its SINR levels within the threshold was an appropriate step to take. It can be observed that restricting the transmit power of the FUE at 18 dBm caused a slight improvement of the data rate of the cell edge MUE user by about 4 Mbps, while the FUE got a degraded service of about 12.5 Mbps in the rate at maximum transmit power. From Fig. 5, the interference generated by FUE remained the same (relatively constant) as against those of MUE showing increased interference levels as distance increased. This shows that with power control, the FUE is not an interferer to the MUE in the uplink.

Without placing any limit on the FUE transmit power, it can be observed from Fig. 6 that FUE was able to achieve 40 Mbps under 10 dB of interference amounting to 11.76 dB in SINR, while the MUE achieved 15 Mbps on a similar interference level at 2.62 dB in SINR value. Without restricting the FUE transmit power to 18 dBm, the MUE at the cell edge suffered from low SINR levels to the range of 0.86 dB as against 2.62 dB in FUE restricted transmit power. It can be observed from Fig. 7 that the implementation of ICR on FUE showed an improvement in the rate from 27.5 Mbps to 30.25 Mbps which amounts to about 3 Mbps of rate gained in the bid to maintain an acceptable SINR threshold of 9 dB for FUE. The ICR action of SINR threshold recovery only caused a slight degradation of the MUE date rate from about 15 Mbps to 14 Mbps (1 Mbps), translating to an SINR level of 0.07 dB.

The FUE values seem to decrease initially from 0 to 40 Mbps, indicating a decline in data rate. At the beginning, FUE is at 0 and gradually increases to 33.5 Mbps and then suddenly drops to 30.5 Mbps at 37 Mbps, showing some fluctuations. Afterward, it continues to decrease, reaching 27.5 at 40 Mbps. The MUE values also show a similar trend to FUE, starting at 2 and gradually increasing to 8.9 at 33.5 Mbps, and then experiencing a significant increase. The MUE then continues to rise from 8.9 to 15.2 at 40 Mbps. Overall, both FUE and MUE initially follow a somewhat linear trend with fluctuations and then show an accelerated increase.
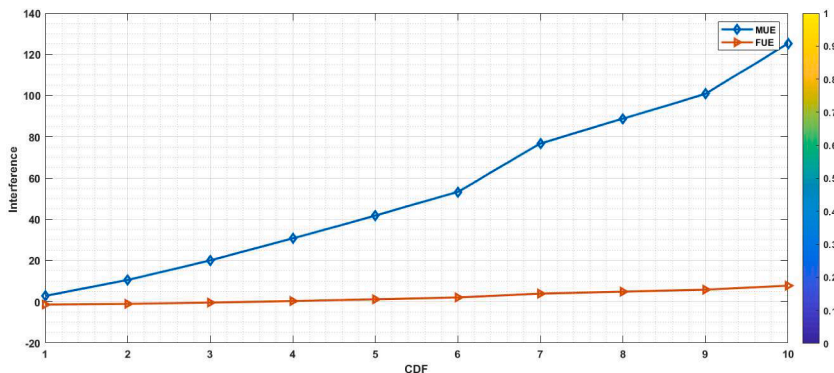

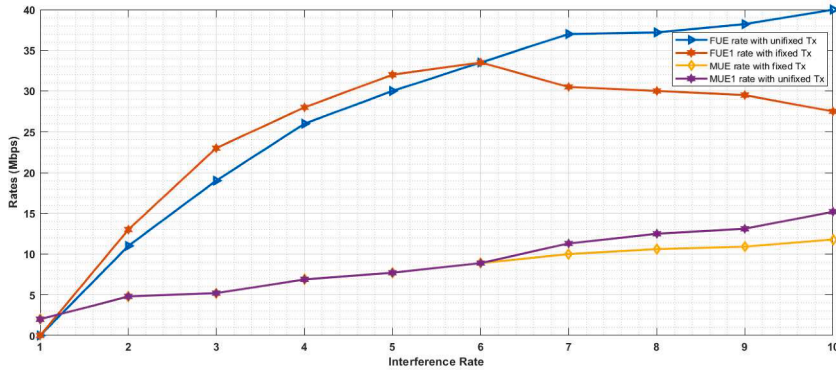**Fig. 5.** MUE and FUE interference levels.
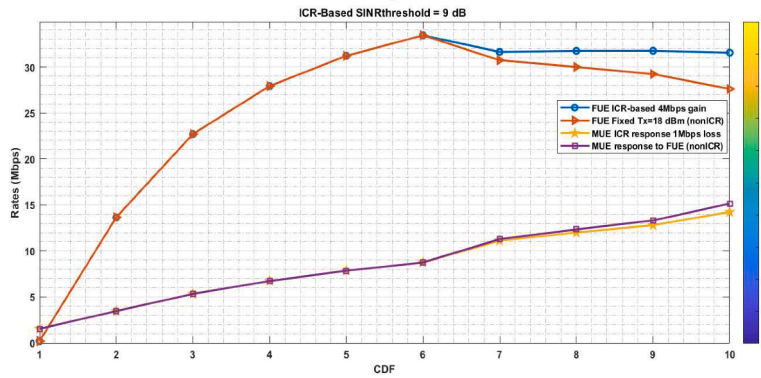
Fig. 6. MUE and FUE interference rate.

Fig. 7. ICR-based rate improvement.

6.3. ICR implementation to power control

The role of the optimization algorithm is to evaluate the initial transmit power when FUE is within the eNB cell, as MUE is already connected. In this way, the FUE allowable transmit power (Txmax) is evaluated by Eq. (4). After the initial evaluation, it becomes unnecessary to carry out re-evaluation, as the optimization equation ensures that the FUE does not become an interferer at the entry point because ITU specified UE Tx power initializing from least possible to maximum allowed in steps of 4 dBm. Hence, the necessity for an ICR-based uplink power control algorithm (ICR-UPCA) that can estimate the cost and benefit of power control within the network. ICR showed the capability of fractional power control, by performing power adjustment of either FUE or MUE with cost and profit estimation for SINR improvement of either user.

Figs. 6 and 7 showed ICR-power level correction such that fractional power change of FUE posed no significant effect on the MUE. Whereas, it is possible to trade signal quality between both network structures. In Fig. 7, 6.67 % was traded in channel capacity to gain 12.5 % which translates to about 4 Mbps and 1 Mbps channel improvement respectively for the MUE at the cell edge. In conclusion,
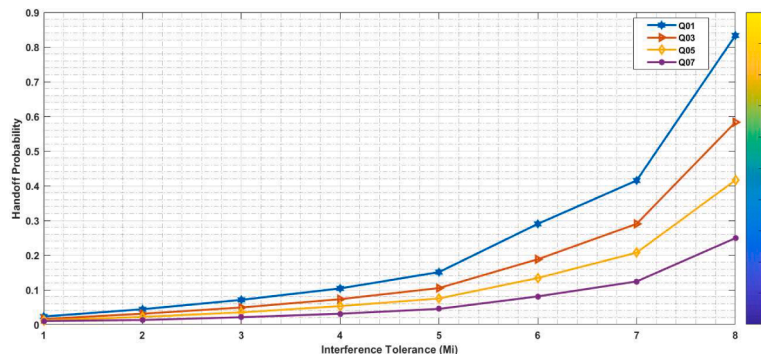

Fig. 8. Handoff probability due to interference tolerance.

ICR-UPCA is effective at critical points where power is essential. It can be seen that the collaboration between the FeNB and MeNB in interference mitigation yielded improved results and ultimately improved the MUE network experience at the cell edge while protecting the femtocell users. The interference contribution rate (ICR) is crucial for UE power adjustment considering other users. It can be used to examine the impact on other users before making adjustments. Fig. 7 illustrates the ICR's impact on macro cell user SINR when adjusting the femtocell SINR target. The amount of loss in data rate as a result of the degraded channel as shown in Fig. 7 was negligible even though the gains of 4 Mbps to FUE were appreciable.

6.4. Signal quality-based handoff algorithm

The handoff algorithm was assessed, and the findings are depicted in Fig. 8. As channel quality improved, the handoff rate decreased, while the network's tolerance to interference increased, especially when transitioning to stronger interferers. The system's handoff algorithm was activated by fluctuations in the Reference Signal Received Quality (RSRQ) indicator, which correlated with interference and path loss. According to the results presented, the handoff probability decreased from 0.83 to 0.58 with improving channel quality. It was observed from the data presented that the power utilization of the macro cell user (MUE) was improved. This was a result of handoffs of higher interferers for better quality channels, as less energy is required for communication. To control handoff rates in the network, UEs are handed off based on the maximum interference contributed.

7. Result validation

The results obtained are validated using the Fractional power control (FPC) scheme [32]. The scheme is introduced and deployed based on path loss compensation [33,34]. The UE makes efforts to transmit at a rate required to overcome path loss by increasing its transmit power according to a set compensation ratio. In Fig. 9, the achieved rate at lower interference levels of MUE by the FPC scheme was observed to be up to 30.7 Mbps at Tx_{max}. Whereas the proposed scheme achieved 11.5 Mbps and 15.1 Mbps when FUE Tx_{max} is limited to 18 dBm. This was so because the FPC did not consider the existence of the FUE as the scheme is focused on overcoming path loss without interference considerations. Also, from the FUE side, the scheme acted as though in isolation. The proposed scheme was better suitable for a coordinated HetNet environment.

In Fig. 10, the FPC scheme generated higher interference signals of about 7.8 dBm, while the proposed scheme generated about 5.5 dBm in simulated results to the FUE which extremely degraded the FUE network. This can be ascribed to its higher data rate recorded in Fig. 9. Whereas the proposed scheme showed good tolerance in coexistence between both networks and was able to balance the demands of each network within available resources. The proposed scheme provided for improved SINR to the cell edge MUE while ensuring that the FUE SINR threshold of 9 dB was protected.

In Fig. 11, the channel capacity of the FUE is depicted, revealing a degradation to approximately 0.2 Mbps. This is in stark contrast to the rates maintained by the ICR-based scheme, which achieves about 40.2 Mbps and 27.3 Mbps for unfixed and fixed Tx_{max}, respectively. The imposition of an 18 dBm maximum power to the FUE demonstrates improved performance compared to the Fixed Power Control (FPC) scheme, especially in a heterogeneous environment (HetNet). The limitations of the FPC scheme become evident in such a setting, as it is solely path loss-driven and lacks consideration for the FUE's location relative to other cells. This oversight results in high interference with its immediate neighbors, as illustrated by the FUE's performance in Fig. 11. The success of the ICR contribution lies in its ability to dynamically adjust the power levels of individual User Equipment (UE) in the network, thereby enhancing Signal-to-Interference-plus-Noise Ratio (SINR) without negatively impacting co-channel users. The capability to assign and reassign SINR thresholds to users, coupled with the optimization of less useful power levels, confers a distinct advantage to the ICR-based scheme.

In terms of eNB power measurements (i.e., ICR-UPCA), the signal strength of the designated base station (eNB) was measured along
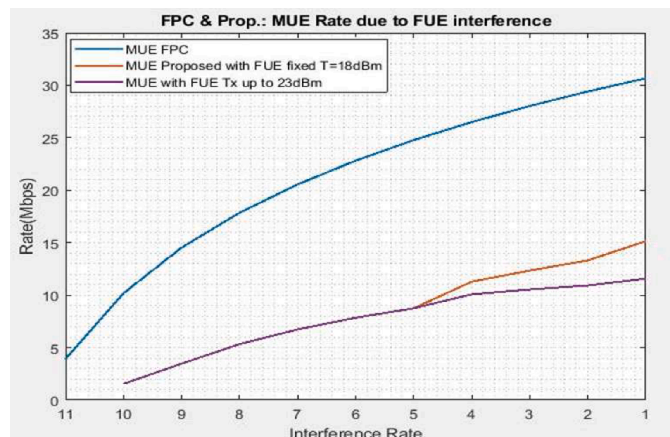

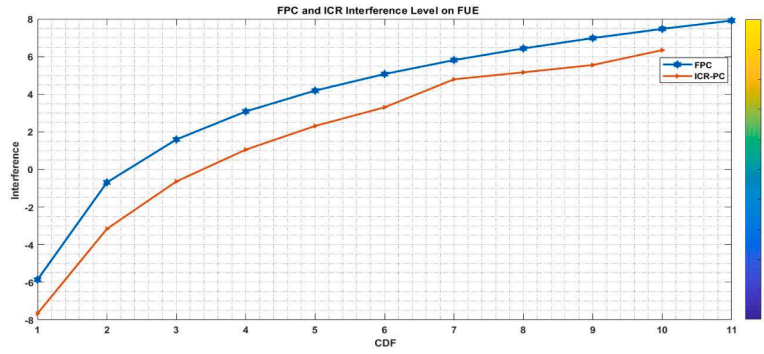**Fig. 9.** MUE rate – FPC and proposed scheme.

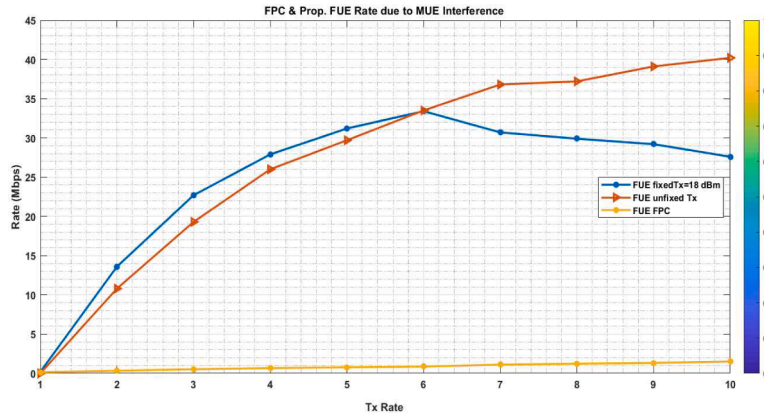**Fig. 10.** FPC and ICR-based interference contribution.

Fig. 11. FUE rate – FPC and proposed scheme.

one of its sectors, ensuring an unobstructed line of sight to mitigate any compromise in results. The primary objective was to identify the cell edge, where handover is most likely to occur. Despite efforts to minimize interference from trees and high-rise buildings, these inevitably served as potential sources of signal reflections. Experimental efforts were made to steer clear of taking measurements in proximity to such structures. Additionally, power lines posed a concern and were unavoidable at specific points. Overall, the acquired results proved reasonably robust for analysis, aligning with the anticipated theoretical power decay constant. Fig. 12 illustrates this trend with distances and their corresponding power levels. The recorded power levels demonstrated the expected decay in signal strength, with some observed fluctuations as the covered distance increased across ten different locations within the same cell and sector.

In Fig. 13, lower power levels were observed near the base station (eNB) tower, aligning with theoretical expectations. Conversely, higher power levels were recorded toward the cell center, gradually decreasing as we moved toward the cell edge, signaling an
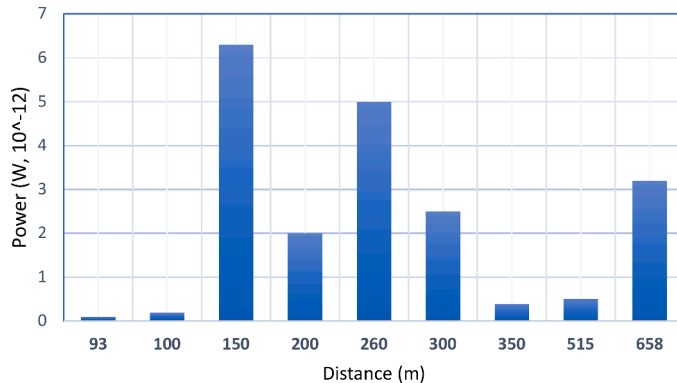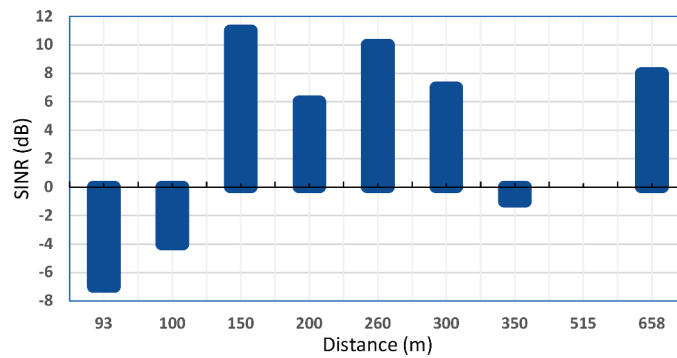

Fig. 12. Measured eNB RSRP.

Fig. 13. Measured eNB SINR.

impending handover. The diminishing signal strength had a noticeable impact on the measured Signal-to-Interference-plus-Noise Ratio (SINR) within the same network. Fig. 13 illustrates this impact, depicting SINR values at distances. The corresponding SINR values were recorded. The degrading signal quality further manifested in the SINR measurements as we approached the cell edge. This phenomenon can be attributed to path loss and various other channel-degrading factors.

At 900 m from the eNB, the handover sequence was triggered. This initiation led to the detection of a signal from an adjacent cell, characterized by superior signal strength compared to the deteriorating signal at the current location. Again, the signal strength at distances of 93 m and 100 m from the base station was notably weak, indicating proximity to the cell's outer boundary. Within the range of 150–300 m, we considered the cell center, signal strength significantly improved, particularly with a clear line of sight, resulting in better signal quality. Expanding beyond this range from 350 m to 658 m, extends to the cell edge, characterized by notably lower signal strength. At the 658 m, there was an overlap in cell signals with adjacent cells, resulting in an inconsistent handoff point. Handoffs occurred randomly around the ±658 m range, indicating an unfixed transition point between cells. Notably, at the point of handoff (658 m or point 9), the recorded signal showed a higher Signal-to-Interference-plus-Noise Ratio (SINR). It appeared evident that the handoff was not initiated due to the slow movement of the testing device toward the 6G cell edge.

Considering UE hardware power utilization analysis, it was observed that hardware subsystems, particularly the UE screen, constituted a significant power consumption point with high energy dissipation. The screen and processors emerged as crucial functional components during the measurements. To maintain simplicity and consistency, the brightness level of the UE screen remained constant throughout the process. A critical aspect of the investigation involved assessing the impact of the UE's processors and graphic processing unit (GPU) system on energy consumption. Table 3 illustrates the processor clocking activities spanning from the center to the edge of the macro cell coverage area. This provides insights into the variations in processor activity across different locations within the coverage area. In terms of UE processor activity, the depicted processor activities in Table 3 revealed instances of elevated processor engagement, particularly notable during services such as video calls and voice-only calls. This heightened activity suggests a potential for increased power utilization. Interestingly, services like video streaming did not exhibit a consistent trend but instead indicated vulnerabilities to path loss, with variations linked to increasing distances toward the cell edge. This distinction in service behavior led to the classification of applications into two categories: real-time and non-real-time applications. Real-time applications, exemplified by video calls and voice-only calls, demonstrated higher processor activities and, consequently, potential for heightened power consumption. On the other hand, non-real-time applications, such as video streaming, displayed susceptibility to path loss variations as distances increased toward the cell edge. Appendix I (a-f) shows the various traffic workload for edge devices (See GitHub code: https://github.com/ken-cisco/ICR-UPCA.cpp.git).

Fig. 14 illustrates notable processor activities during idle mode at the cell center and cell edge (idle C & E). Notably, at the cell edge, the second half of the quad-core processors exhibited higher engagement, whereas similar responses were observed at the cell center, resulting in an average distinction in response. During the voice call application (voice call. E & C), identical readings were recorded for all 8 processor clocks at both cell edge and center. Distinct processor clocking activities were observed during the video streaming application (video stream E & C). However, there was no significant difference between these activities due to the relatively consistent clocking response from cell edge to cell center, with an alternation of highly clocked processor sets.

At the cell center, the first 4 sets of processors ran at lower clocking speeds compared to the other 4, while at the cell edge, the first 4 sets were clocked higher, and the other 4 were clocked lower. Nevertheless, this did not substantiate the argument of processor-induced additional power utilization from the center to the edge of the macro cell network. Examining the video call application from cell center to cell edge (video call E.C), higher processor clocking was observed compared to other applications mentioned earlier. However, an alternation of processor clocking from the first four sets to the others indicated that processor activities did not significantly change from cell center to cell edge, thus not justifying any difference in energy utilization during power measurement and analysis. The maximum power utilized by the processor was not considered in the analysis due to manufacturer restrictions. The UE power, as presented in Table 2 and depicted in Fig. 15, revealed spikes in power utilization during real-time service deployment. The offline and online power during UE idle mode correlated with the distance covered toward the cell edge. Online video stream and offline voice call services generated distinct power levels within the same network environment and coverage distance. Notably, online video call streaming utilized distinct power levels higher than any other deployed application by the user equipment (UE). This

Table 3
Measured processor clocking.

Voice call Edg/Ctr	Video call Ctr	Video call Edg	Video stream Ctr	Video stream Edg	Idle Edg	Idle Ctr
793	1807	1729	1209	1547	962	793
1027	1807	1729	1209	1547	962	793
1027	1807	1729	1209	1547	793	793
1027	1807	1729	1209	1547	793	884
1547	1729	1807	1456	1144	1378	1040
1547	1729	1807	1456	1144	1378	1040
1547	1729	1807	1495	1144	1378	1040
1547	1729	1807	1495	1144	1378	1040
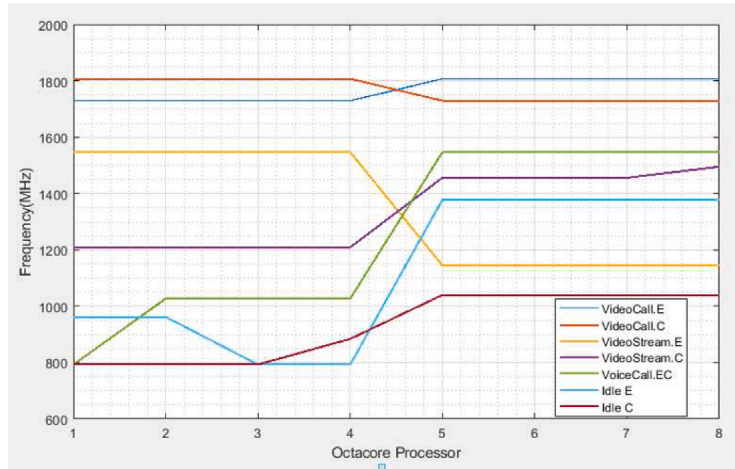
Fig. 14. Measured processor clocking.
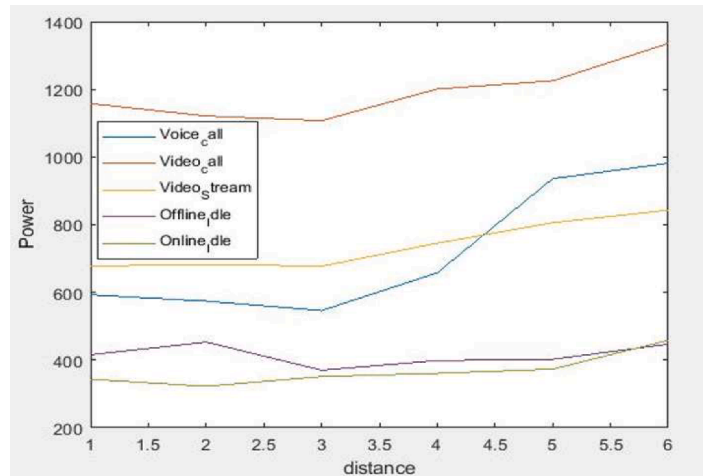
Fig. 15. UE power levels per deployed application.

observation led to the categorization of power levels into Real-time (RT) and non-Real time (nRT) in updating the ICR table.

8. Discussion

Essentially, the power optimization model in Eq. 4 was used to determine the FUE Tx$_{max}$. For every MUE Tx power that generates interference levels above the FUE tolerance band, the ICR was determined with further analysis in Appendix A. Eqs. 7 and 8 was deployed for ICR and SINR threshold determination. The ICR-based power control was applied to determine the rate of interference

suffered by users and the extent of power adjustment required. ICR evaluation was carried out on both FUE and MUE, this made it possible to understand the interference status of every user while balancing the rates gained within the shared channel. It becomes easier to protect the FUE while maintaining an improved cell edge user channel quality. Using the optimization equation in Eq. 4, the maximum Tx evaluated for MUE and FUE was 200 mW and 191 mW respectively. From simulations done, FUE becomes an interferer to MUE only at Tx power of about 51 mW and above. The maximum data rate achievable by FUE and MUE at the cell edge was possibly controlled at 27.5 Mbps for fixed Tx power at 18 dBm and 15 Mbps respectively, as SINR was maintained at 15 dB for FUE and 1 dB for MUE. The two identified contributions of the proposed scheme are:

- Improved SINR Levels: The implementation of the Interference Contribution Rate-based Uplink Power Control Algorithm (ICR-UPCA) led to a substantial improvement in SINR levels for users at the cell edge. This dynamic adjustment of uplink power effectively mitigated interference, resulting in enhanced signal quality.
- Efficient Handoffs: The Handoff Algorithm based on Reference Signal Received Quality (RSRQ) significantly improved the efficiency of handovers between cells. This optimization contributed to higher SINR levels during transitions, ensuring uninterrupted service for users on the move.

8.1. Limitation

Though the proposed power control algorithm introduces a cooperative approach between edge nodes to achieve an advantage on the shared spectrum, the identified implementation concerns are highlighted below.

  i. In such advanced power control algorithm, this may provide difficulties because of their intricate computational structure, which makes decision-making and implementation more difficult.
 ii. Regardless of the energy optimization benefits, this could use a lot of processing power especially in complex workloads, negating any potential energy savings.
iii. Controlling device interference in dense networks is difficult and affects algorithm performance.
 iv. Furthermore, the computing needs of these algorithms large scale Cyber-physical environment may introduce intrinsic latency in communication, (which will impact real-time applications where delay is critical, e.g., remote operations and autonomous cars).
  v. In 5G/6G networks, reduced computing complexity may limit accuracy, scalability, flexibility, and security issues while also stifling innovation.

Similar to the work [34], the proposed power control algorithm is limited to low-complexity power control. It is useful in scenarios where frequency reuse factors do not apply, and there is the coexistence of network hierarchical structures that could cause Inter-cell interference (ICI). Although the work [35] addressed the issue of efficient power control in heterogeneous networks using deep learning, the downside is the high computational complexity for edge-connected connections. As such the work [36], used a joint power allocation approach and employed fast evolutionary algorithm. The proposed scheme lacks multi-agent deep reinforcement learning approach to handle complexities caused by ICI. It only supports spectrum sharing and coexistence between nodes with different network structures. Overall, the utilization of the multi-agent deep reinforcement learning (DRL) algorithm, as well as related concepts found in [34–37], can be explored to solve the problems, with tradeoffs that highlight computational complexities during handoff.

9. Conclusion

In this paper, we studied an effective approach to the problem of suboptimal Signal-to-Interference-plus-Noise Ratio (SINR) experienced by macro cell users at the cell edge, even within a femtocell network. The objective is to effectively utilize the 5G-NR radio spectrum for user data transmission while minimizing overhead. The increasing interference levels require a cohesive approach that combines network infrastructures and interference control. In this paper, user services are categorized into real-time and non-real time, which is essential for customizing SINR improvement efforts. Two innovative solutions are developed. First, Interference Contribution Rate-based Uplink Power Control Algorithm (ICR-UPCA), which dynamically adjusts uplink power levels based on real-time interference, effectively mitigating interference and elevating SINR. Second, Handoff Algorithm based on Reference Signal Received Quality (RSRQ) was introduced to optimize handovers between cells to further enhance SINR and service quality. The proposed handoff-mechanisms showed an improved performance with lower Computational complexity, better quality of service, optimal utilization of the 5G-NR radio spectrum. These contribute to a more robust and optimized 5G-NR network, while ensuring satisfactory user experience. Future work will focus on implementing ICR-UPCA within a HetNet network i.e., Heterogeneous Cyber-Physical Networks (HCPNs) deployed in the context of 6G-NR. Also, conducting an in-depth investigation on the security limitations inherent in the edge nodes within a functional femtocell infrastructure for closed subscriber group mode (CSG) will be carried out. An investigation on RSRQ-based handoff algorithm using Reinforcement learning (RL) to predict and minimize interference patterns will be explored. The other future applications are advanced game theory, evolutionary algorithms, federated learning, and Multi-Agent Systems (MAS) using heuristic optimization algorithms (i.e.., ant colony optimization and simulated annealing. Ultimately, the aim is to develop a multi-facted hybrid model that will provide optimal interference management and uplink power control solutions in 6G

edge cells within HCPNs by integrating various AI techniques.

Financial support

CRediT authorship contribution statement

Declaration of Competing Interest

The authors declare that they have no known competing financial interests or personal relationships that could have appeared to influence the work reported in this paper.

Data availability

The Code scripts for data generation are publicly available in the GitHub repository as part of this research: https://github.com/ken-cisco/ICR-UPCA.cpp.git.

Acknowledgment

Supplementary materials

Supplementary material associated with this article can be found, in the online version, at doi:10.1016/j.iot.2023.101031.

Appendix A

(a) Derived Parameters for Uplink Power Control Algorithm and Interference Contribution Rate.

Pf	0.048	6.50	18.68	33.85	50.56	68.14	104.74	123.45	142.39	180.69
Prf	0.0151	2.0166	5.7085	10.2483	15.1668	20.3082	30.6903	34.2014	38.0508	46.7794
Imf	2.0545	5.7955	10.3444	15.3073	20.4404	25.7086	36.1844	39.4487	43.1522	51.7786
SINRf	0	1.1252	2.8161	5.1030	6.8556	9.2393	11.8194	12.1986	14.0539	15.3192
SINRm	0.122	0.2711	0.4466	0.5940	0.7221	0.8332	1.0102	1.0756	1.1318	1.2297
Ifm	0.0013	0.1564	0.4441	0.7843	1.1565	1.5500	2.3686	2.7605	3.1474	3.9486
Prm	0.3546	0.8989	1.6096	2.3429	3.1171	3.9245	5.5853	6.3681	7.1388	8.7413
Pm	6.55	18.68	33.85	50.56	68.14	86.26	123.49	142.39	161.48	200.00

(a) FUE Tx power restricted to 18 dBm (68.14 mW)

Pf	0.048	6.50	18.68	33.85	50.56	68.14	68.14	68.14	68.14	68.14
Prf	0.0151	2.0166	5.7085	10.2483	15.1668	20.3082	19.98	18.88	18.22	17.65
Imf	0.3424	0.9659	1.7241	2.5512	3.4067	4.2848	6.0307	6.5748	7.1920	8.6298
SINRf	0.0137	1.5754	3.8247	5.9270	7.6995	9.1527	7.4140	6.9996	6.5823	5.7796
SINRm	0.1122	0.2710	0.4466	0.5940	0.7221	0.8332	1.1858	1.3520	1.5157	1.8559
Ifm	0.0013	0.1564	0.4441	0.7843	1.1565	1.5500	1.5500	1.5500	1.5500	1.5500
Prm	0.3546	0.8989	1.6096	2.3429	3.1171	3.9245	5.5853	6.3681	7.1388	8.7413
Pm	6.55	18.68	33.85	50.56	68.14	86.26	123.49	142.39	161.48	200.00

(a) ICR Table

Pf	0.048	6.50	18.68	33.85	50.56	68.14	73.16	78.19	83.21	93.26
Prf	0.0151	2.0166	5.7085	10.2483	15.1668	20.3082	19.98	18.88	18.22	17.65
Imf	0.3424	0.9659	1.7241	2.5512	3.4067	4.2848	6.0307	6.5748	7.1920	8.6298
SINRf	0.0137	1.5754	3.8247	5.9270	7.6995	9.1527	7.9602	8.0320	8.0382	7.9101
SINRm	0.1122	0.2710	0.4466	0.5940	0.7221	0.8332	1.1601	1.2974	1.4279	1.6817
Ifm	0.0013	0.1564	0.4441	0.7843	1.1565	1.5500	1.6545	1.7484	1.8393	2.0380
Prm	0.3546	0.8989	1.6096	2.3429	3.1171	3.9245	5.5853	6.3681	7.1388	8.7413
Pm	6.55	18.68	33.85	50.56	68.14	86.26	123.49	142.39	161.48	200.00

(a) IoT 6G edge Network Performance Metrics at Different Distances

S/N	Distance (m)	Power 10–13W	Power (dB)	RSRP (dBm)	RSRQ (dB)	RSSNR (dB)	ASU (dBm)	SINR (dB)
1.	93	1.0	−130	−100	−10	1.7	40	−7
2.	100	1.9	−127	−97	−9	7.2	43	−4
3.	150	63.0	−112	−82	−10	12.7	58	11
4.	200	20.0	−117	−87	−9	9.7	53	6
5.	260	50.0	−113	−83	−9	12.5	57	10
6.	300	25.0	−116	−86	−10	5.0	54	7
7.	350	3.9	−124	−94	−17	−0.3	46	−1
8.	515	5.0	−123	−93	−14	−0.5	47	0
9.	658	32.0	−115	−85	−10	2.5	55	8

(a) IoT Power Consumption of Various Activities at Different Distances in a 6 G Edge Network

S/N	Distance (m)	Voice call (mW)	Video call (mW)	Video stream (mW)	Online idle (mW)	Offline idle (mW)
1.	35	352.7	1157.7	677.6	415.4	343.3
2.	85	328.5	1121.3	682.7	453.3	322.5
3.	180	366.6	1107.5	677.3	370.1	351.4
4.	360	420.1	1200.8	745.4	398.5	360.9
5.	515	444.1	1225.3	806.0	402.3	373.3
6.	645	582.9	1335.5	843.1	446.9	458.3

(a) Power Consumption workload at edge user Communication without online idle states

S/N	Distance (m)	Voice call (mW)	Video call (mW)	Video stream (mW)
1.	35	9.4	96.9	43.6
2.	85	6.0	22.6	48.7
3.	180	15.2	92.0	43.3
4.	360	59.2	156.9	111.4
5.	515	70.8	177.6	172.0
6.	645	124.6	243.2	209.1

References

[1] Z.J. Ali, N.K. Noordin, A. Sali, F. Hashim, Fair Energy-Efficient resource allocation for downlink NOMA heterogeneous networks, IEEE Access 8 (2020) 200129–200145, https://doi.org/10.1109/ACCESS.2020.3035212.

[2] S.H. Kim, S.Y. Park, K.W. Choi, T.-J. Lee, D.I. Kim, Backscatter-aided cooperative transmission in wireless-powered heterogeneous networks, IEEE Trans. Wirel. Commun. 19 (11) (2020) 7309–7323, https://doi.org/10.1109/TWC.2020.3010544. November.

[3] S. Manzoor, M.A. Kayani, N. Ali, N.I. Ratyal, H.G. Mohamed, TiWA: achieving tetra indicator Wi-Fi associations in software defined Wi-Fi networks, IEEE Access 11 (2023) 89520–89534, https://doi.org/10.1109/ACCESS.2023.3307476.

[4] R. Kurda, Heterogeneous networks: fair power allocation in LTE-A uplink scenarios, PLoS ONE 16 (6) (2022), e0252421, https://doi.org/10.1371/journal.pone.0252421. Article.

[5] K.C. Okafor, B. Adebisi, K. Anoh, Lightweight multi-hop routing protocol for resource optimization in edge computing networks, Internet Things 22 (2023).

[6] M.N. Alam, R. Jäntti, Z. Uykan, Hopfield neural network based uplink/downlink transmission order optimization for dynamic indoor TDD femtocells, IEEE Access 11 (2023) 85414–85425, https://doi.org/10.1109/ACCESS.2023.3300588.

[7] G. Alsuhli, et al., Mobility load management in cellular networks: a deep reinforcement learning approach, IEEE Trans. Mobile Comput. 22 (3) (2023) 1581–1598, https://doi.org/10.1109/TMC.2021.3107458. Pages1 March.

[8] W. Du, et al., Weighted sum-rate and energy efficiency maximization for joint ITS and IRS assisted multiuser MIMO networks, IEEE Trans. Commun. 70 (11) (2022) 7351–7364, https://doi.org/10.1109/TCOMM.2022.3213356. PagesNov.

[9] S.C. Chan, H.C. Wu, C.H. Ho, L. Zhang, An augmented Lagrangian approach for distributed robust estimation in large-scale systems, IEEE Syst. J. 13 (3) (2019) 2986–2997, https://doi.org/10.1109/JSYST.2019.2897788. Sept.

[10] J. Turka, M.D.V. Olivia, S. Foo, Optimization of LTE uplink performance in multivendor heterogeneous networks, in: International Conference on Information Networking (ICOIN), Chiang Mai, Thailand, 2018, pp. 374–379.

[11] E. Kazemi, F. Taherkhani, L. Wang, Semisupervised learning for noise suppression using deep reinforcement learning of contrastive features, IEEE Sens. Lett. 7 (4) (2023) 1–4, https://doi.org/10.1109/LSENS.2023.3264998. Pages.

[12] Y. Chen, Z. Wang, Z. Liu, Resource allocation and power control based on noncooperative game for D2D communications underlaying cellular networks, Wirel. Pers. Commun. 124 (2022) 2723–2733.

[13] L. Li, C. Yang, M.E. Mkiramweni, L. Pang, Intelligent scheduling and power control for multimedia transmission in 5G CoMP systems: a dynamic bargaining game, IEEE J. Sel. Areas Commun. 37 (7) (2019) 1622–1631, https://doi.org/10.1109/JSAC.2019.2916491. Pages.

[14] A. Srivastava, et al., Enhanced distributed resource selection and power control for high frequency NR V2X Sidelink, IEEE Access 11 (2023) 72756–72780, https://doi.org/10.1109/ACCESS.2023.3295822, 2023Pages.

[15] W. Kim, Z. Kaleem, K. Chang, Interference-aware uplink power control in 3GPP LTE-A HetNet, Wirel. Pers. Commun. 94 (2017) 1057–1071, https://doi.org/10.1007/s11277-016-3669-y.

[16] G.T.S. Krishna, R. Madhu, A utility function based uplink power control algorithm in LTE-advanced networks, in: IEEE International Conference on Communication and Signal Processing, 2016. April 6-8.

[17] X. Cai, I.Z. Kovacs, J. Wigard, P.E. Mogensen, A centralized and scalable uplink power control algorithm in low SINR scenarios, IEEE Trans. Veh. Technol. 70 (9) (2021) 9583–9587, https://doi.org/10.1109/TVT.2021.3097773.

[18] K. Sun, Y. Yan, W. Zhang, Y. Wei, An interference-aware uplink power control in LTE heterogeneous networks, in: TENCON 2018 - IEEE Region 10 Conference, Jeju, Korea (South), 2018, pp. 0937–0941. Pages.

[19] K.C. Ting, W.Y. Lin, C. Wang, Loading Aware Green Power Control (LAGPC) For the Mitigation of Co-tier Downlink Interference for Femtocell in Future 5G Networks, 24, Mobile Networks and Applications, 2019, pp. 864–877. Pages.

[20] B. Shen, Z. Lei, X. Huang, Q. Chen, An interference contribution rate based small cells on/off switching algorithm for 5G dense heterogeneous networks, IEEE Access 6 (2018) 29757–29769, https://doi.org/10.1109/ACCESS.2018.2841044.

[21] B. Feng, et al., HetNet: a flexible architecture for heterogeneous satellite-terrestrial networks, IEEE Netw. 31 (6) (2017) 86–92, https://doi.org/10.1109/MNET.2017.1600330.

[22] Z. Gong, X.S. Shen, C. Li, Y. Song, R. Su, High-accuracy positioning services for high-speed vehicles in wideband mmwave communications, IEEE Trans. Signal Process. 71 (2023) 3867–3882, https://doi.org/10.1109/TSP.2023.3324727.

[23] W. Chaowei, W. Ziye, X. Lexi, Y. Xiaofei, Z. Zhi, W. Weidong, Collaborative caching in vehicular edge network assisted by cell-free massive MIMO, Chinese J. Electron. 32 (6) (2023) 1218–1229, https://doi.org/10.23919/cje.2022.00.294.

[24] J. García-Morales, G. Femenias, F. Riera-Palou, Statistical analysis and optimization of a fifth-percentile user rate constrained design for FFR/SFR-aided OFDMA-based cellular networks, IEEE Trans. Veh. Technol. 67 (4) (2018) 3406–3419, https://doi.org/10.1109/TVT.2017.2782943.

[25] I. Budhiraja, S. Tyagi, S. Tanwar, N. Kumar, J.J.P.C. Rodrigues, DIYA: tactile internet driven delay assessment NOMA-based scheme for D2D communication, IEEE Trans. Ind. Inform. 15 (12) (2019) 6354–6366, https://doi.org/10.1109/TII.2019.2910532. Dec.

[26] Q. Xue, R. Wei, S. Ma, Y. Xu, L. Yan, Multi-user mmwave uplink communications based on collaborative double-RIS: joint beamforming and power control, IEEE Commun. Lett. 27 (10) (2023) 2702–2706, https://doi.org/10.1109/LCOMM.2023.3309710.

[27] A. Subhash, A. Kammoun, A. Elzanaty, S. Kalyani, Y.H. Al-Badarneh, M.-S. Alouini, Optimal phase shift design for fair allocation in RIS-aided uplink network using statistical CSI, IEEE J. Selected Areas Commun. 41 (8) (2023) 2461–2475, https://doi.org/10.1109/JSAC.2023.3288266.

[28] E. Shi, J. Zhang, D.W.K. Ng, B. Ai, Uplink performance of RIS-aided cell-free massive MIMO system with electromagnetic interference, IEEE J. Selected Areas Commun. 41 (8) (2023) 2431–2445, https://doi.org/10.1109/JSAC.2023.3288265.

[29] Q. Li, et al., Achievable rate analysis of the STAR-RIS-aided NOMA uplink in the face of imperfect CSI and hardware impairments, IEEE Trans. Commun. 71 (10) (2023) 6100–6114, https://doi.org/10.1109/TCOMM.2023.3287995.

[30] Liming Yang, Honglin Hu, Ting Zhou, Tianheng Xu, Joint coded caching and BS sleeping strategy to reduce energy consumption in 6G edge networks, Internet Things 24 (2023), https://doi.org/10.1016/j.iot.2023.100915.

[31] Seyed Hosein Mousavi, Jafar Pourrostam, Mahdi Nangir, Low computational complexity joint iterative detection and decoding without ARQ in massive MIMO systems with UAVs, Comput. Commun. 192 (2022) 279–288, https://doi.org/10.1016/j.comcom.2022.06.009.

[32] A.D. Firouzabadi, A.M. Rabiei, M. Vehkaperä, Fractional frequency reuse in random hybrid FD/HD small cell networks with fractional power control, IEEE Trans. Wireless Commun. 20 (10) (2021) 6691–6705, https://doi.org/10.1109/TWC.2021.3075987.

[33] K.C. Okafor, B. Adebisi, A.O. Akande, K. Anoh, Agile gravitational search algorithm for cyber-physical path-loss modelling in 5G connected autonomous vehicular network, Veh. Commun. (2023), https://doi.org/10.1016/j.vehcom.2023.100685.

[34] T.M.T. Nguyen, T.V. Nguyen, W. Noh, S. Cho, Energy-efficient and low-complexity transmission control with SWIPT-NOMA for green cellular networks, IEEE Trans. Wireless Commun. 22 (10) (2023) 6673–6690, https://doi.org/10.1109/TWC.2023.3244968.

[35] L. Zhang, J. Peng, J. Zheng, M. Xiao, Intelligent cloud-edge collaborations assisted energy-efficient power control in heterogeneous networks, IEEE Trans. Wireless Commun. 22 (11) (2023) 7743–7755, https://doi.org/10.1109/TWC.2023.3255216. Nov.

[36] S.K. Goudos, et al., Joint QoS aware admission control and power allocation in NOMA downlink networks, IEEE Access 11 (2023) 30873–30887, https://doi.org/10.1109/ACCESS.2023.3262117.

[37] Y. Lu, B. Ai, Z. Zhong, Y. Zhang, Energy-efficient task transfer in wireless computing power networks, IEEE Internet Things J. 10 (11) (2023) 9353–9365, https://doi.org/10.1109/JIOT.2022.3223690, 1 1.